Multispectral mixing scheme for smart LED-based lighting system

Song-Bor Chiang*[a], Ming-Chin Chien[a] and Chung-Hao Tien[b]
[a]Department of Photonics and Institute of Electro-Optical Engineering, National Chiao Tung University, 1001 Ta-Hsueh Road, Hsinchu 30010, Taiwan
[b] Department of Photonics and Display Institute, National Chiao Tung University, 1001 Ta-Hsueh Road, Hsinchu, 30010, Taiwan

ABSTRACT

LED cluster is probably the most relevant among the emerging solid-state lighting techniques. Impressive scenarios of a wide range of color quality and luminous efficiency have been obtained, mostly at the condition of constant ambient temperature. This paper removes the constraint in ambient temperature. We present a methodology analogous to a general lens design rule to optimize step-by-step the spectral power distribution of a white-light LED cluster. The scheme enables the users to determine the optimal operation to meet requirements such as light efficiency, color quality, or other figures of merit over a wide range of color temperatures. All main factors influencing the spectral power distribution (SPD) are discussed, alongside the implementation of a pentachromatic R/G/B/A/CW platform suitable for clinic use. The result shows the multispectral cluster can be modulated within the color temperature from 2800K to 8000K in the range ambient temperature (10^{o}C ~ 100^{o}C) with high color quality scale (CQS > 85 points) and the possibly highest luminous efficiency.

Keywords: Cluster, LEDs mixing optimization, lens design, color rendering, luminous efficiency, CQS, merit function, chromaticity point.

1. INTRODUCTION

Light-emitting diode (LED) technology has profoundly changed the way light is generated across a wide field of applications due to its unique characteristics, including possibly the highest optoelectronic conversion efficiency, the capability of modulating spectral composition and environmentally benign raw materials [1]. Among these features, one challenge in the design of a LED-based cluster is how to adjust the spectral power distribution (SPD) in an underdetermined condition, thus enabling us to manipulate strategically the chromaticity point, light quality, and system efficiency according to different operational purposes. For example, we are able to enhance the fidelity appearance in high-color-quality mode or to employ higher efficiency at a sacrifice of color rendering in an unoccupied area [2].

Generally, the mixing question for a white LED cluster can be separated into three aspects:

(a) Energy–the most widespread figures of merit from the viewpoint of energy are the luminous efficacy of radiance (LER) and the luminous efficiency (LE). The LER represents the amount of luminous flux (lumen) converted from a per-unit optical power (watt), whereas the LE is defined as the luminous flux normalized to the electrical input power (watt) expended to operate the LED. In principle, the LE is the product of the LER and electric-to-optical power conversion efficiency [3].

(b) Light quality–the major characteristic of white light quality is its ability to reproduce colors of illuminated objects with high fidelity. The CRI proposed by the CIE (Commision Internationale de l'Éclairage) is the most widely recognized figure of merit. However, CRI has been criticized for its lack of fidelity in ranking sources, especially those with highly peaked spectra such as LEDs [4]. As a consequence, numerous refinements are being explored, such as the color quality scale (CQS) [5], gamut area index (GAI) [6], and color saturation index (CSI) [7].

(c) Mixing scheme—the SPD of an LED cluster can be synthesized by using (i) additive mixing of two or more single-color LED chips (LED-primary-based approach), (ii) wavelength-conversion via using phosphors or other materials (LED-plus-phosphor-based approach), and (iii) a hybrid approach composed of (i) and (ii) [8].

The prior SPD optimizations were addressed mainly via multiple single-color LEDs and usually had been restricted to certain specific conditions, such as CRI, LER, and so forth [9]. Although several cases using a hybrid approach have

Light-Emitting Diodes: Materials, Devices, and Applications for Solid State Lighting XVI,
edited by Klaus P. Streubel, Heonsu Jeon, Li-Wei Tu, Norbert Linder, Proc. of SPIE Vol. 8278,
82780D · © 2012 SPIE · CCC code: 0277-786X/12/$18 · doi: 10.1117/12.907834

been proposed for color temperature adaptable systems [10,11]. In this paper, we make an attempt to borrow design techniques from a conventional lens system and offer a solution with wider operation windows to cover aforementioned environments. Our ultimate goal is to develop a general LED design procedure in a more complete treatment. The design flow in all respects can be closely analogous to a conventional lens design process that has long been developed, by which the SPD of an LED cluster can be optimized by going through every step of the modeling. The modeling also considers the dependences of temperature and current as well as the modulation methodology of the SPD. Our merit is based on achieving an acceptable requirement of the color quality scale (CQS) and maximizing the luminous efficiency (LE) over a wild range of color temperature (T_c) and ambient temperature (T_a). Where the CQS is a refinement of general color rendering index (R_a) introduced by the CIE and LE is a practical efficiency merit defined as the luminous flux normalized to the electrical input power (watt) expended to operate the LED, accordingly.

2. CONCEPT OF DESIGN PROCEDURE

First, we emulate a single-color LED as a singlet, whose light-bending power determined by its curvature and refractive index can be conceptually analogous to the emitting luminous flux of an LED determined by the driving current and LE, respectively. As we mix a number of LEDs, the additive mixing by two single-color LEDs is equivalent to two singlet lenses. Likewise, the LED-plus-phosphor-based approach can be regarded as a cemented doublet (dichromatic) or triplet (trichromatic), depending on the number of emitting peak wavelengths. The concept is schematized in figure 1. Based on the hypothesis outlined above, the SPD synthesis can be transformed into a classic lens design problem. For example, an LED cluster composed of red/cool-white/cool-white/green (R/CW/CW/G) is logically equivalent to a double Gauss lens system. The fundamental constraint such as diffraction limitation of a lens system is viewed accordingly as the theoretical boundary of the LER or CRI.

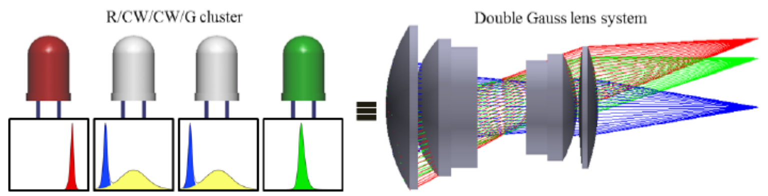

Spectral synthesizing design	Conventional lens design
LED	Lens
Luminous flux	Bending power
Driving current	Lens curvature
Luminous efficiency	Refraction index
Peak wavelength	Abbe number
Full-width at half-maximum	Thickness of Lens
Correlated color temperature	Field angle
LED-primary based approach	Singlet
LED-plus-phosphor based approach	Doublet, triplet, …
Merit: LER, LE, CRI, CQS, …	Aberration: Seidel, Zernike,…
Analysis: e.g., $C_{1/0}$* vs. T_{cc}	Analysis: e.g., MTF vs. field
Tolerance: e.g., degradation vs. merits	Tolerance: e.g., tilt vs. aberrations

Figure 1 Conceptual analogy between the SPD synthesis and conventional lens design. An LED cluster composed of R/CW/CW/G can be regarded as a double Gauss lens system with two singlet lenses and two cemented doublets, where the CW LED is caused by dichromatic mixing.

The solution of a lens design is a typical inverse problem. Given the effective focal length (EFL) and degree of correction for an optical system, it is always possible to determine the curvatures, thicknesses, and number of lenses in sequence. For example, if we aim to design a lens system with a specified EFL and correct three Seidel aberration coefficients, it can be resolved analytically by a set with two singlet lenses; that leaves four degrees of freedom–two powers and two shape factors [the shape factor is defined as $(R_2 + R_1)/(R_2-R_1)$, where R_1 and R_2 are the radii of the first and second surfaces, respectively]. Since the complexity of multiple lenses would increase the computational cost, a more efficient method in lens design would resort to an iterative process, as shown in figure 2(a).

Similarly, we adopt this idea by replacing the lens set with a number of LEDs for certain predefined environments, as proposed in Fig. 2(b). The design procedure includes six steps: (2.1) initial system, (2.2) define boundary condition, (2.3) optimization, (2.4) aberration or merit analysis, (2.5) judgment, and (2.6) tolerance analysis.

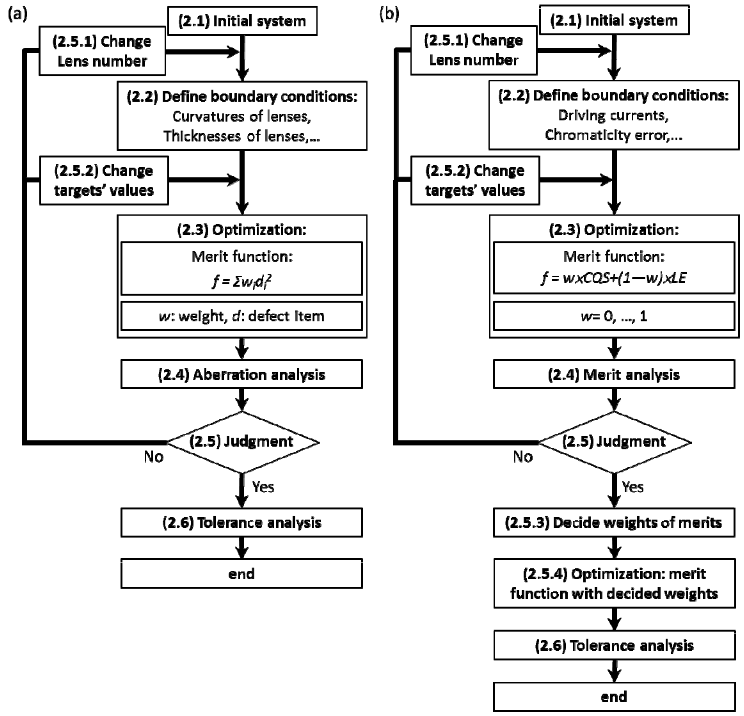

Figure 2 (a) Conventional lens design process and (b) spectral synthesizing design procedure. Both flow charts include six steps: (1) initial system, (2) define boundary condition, (3) optimization, (4) aberration or merit analysis, (5) judgment, and (6) tolerance analysis.

3. OPTIMIZATION

3.1 Spectral modeling

A Gaussian function has been utilized in the incorporation of the spectral power (P), peak wavelength (λ_0) and spectral width ($\Delta\lambda$) with junction temperature. Here we simply select the basic form of double Gaussian function but generalize the relations of all parameters to both junction temperature and drive current. For a pre-recorded spectral database matrix $\mathbf{S}$, the estimated spectral matrix $\hat{\mathbf{S}}$ for a single-color spectrum can be modeled as:

$$\hat{\mathbf{S}} = \mathbf{G} + \mathbf{G}^* \tag{1}$$

where $\mathbf{G} = (\mathbf{g}_1,\ldots,\mathbf{g}_M)^T$ and $\mathbf{G}^* = (\mathbf{g}_1^*,\ldots,\mathbf{g}_M^*)^T$ are M x N Gaussian spectral matrices with M estimated spectra sampled by N points. We could omit $\mathbf{G}^*$ and focus on $\mathbf{G}$ due to the same treatment from Eq. (2)-(5). The matrix $\mathbf{G}$ has M spectral vectors $\mathbf{g}$ with N sampling wavelengths. For the nth point of mth row vector $\mathbf{g}_m$, g_{mn}, its value can be accounted by:

$$g_{mn} = p_m \exp[-(\lambda_n - \lambda_{0,m})^2 / \Delta\lambda_m^{\,2}] \tag{2}$$

The parameters p_m, $\lambda_{0,m}$, and $\Delta\lambda_m$ refer to the mth power, peak wavelength, and spectral width, respectively, whose values could be found by satisfying the following minimization :

$$\arg\min[\ |\mathbf{s}_m - \hat{\mathbf{s}}_m|^2,\ \{p_m,\ \lambda_{0,m},\ \Delta\lambda_m,\ p_m^*,\ \lambda_{0,m}^*,\ \Delta\lambda_m^*\}] \tag{3}$$

where $\mathbf{s}_m$ and $\hat{\mathbf{s}}_m = \mathbf{g}_m + \mathbf{g}_m^*$ are the mth row vectors of $\mathbf{S}$ and $\hat{\mathbf{S}}$, respectively. After solving whole rows we have three M x 1 vectors $\mathbf{p}$, $\boldsymbol{\lambda}_0$, and $\boldsymbol{\Delta\lambda}$ that can empirically be related to junction temperature vector $\mathbf{t}$ and drive current vector $\mathbf{i}$:

$$\ln(\mathbf{p}) = \mathbf{M}_p\mathbf{c}_p\ ,\ \ \boldsymbol{\lambda}_0 = \mathbf{M}_\lambda\mathbf{c}_\lambda \ \text{ and } \ \ln(\boldsymbol{\Delta\lambda}) = \mathbf{M}_{\Delta\lambda}\mathbf{c}_{\Delta\lambda} \tag{4}$$

where $\mathbf{M}_p = [\mathbf{t}^T \ln(\mathbf{t})\ \ \ln(\mathbf{i})\ \ \mathbf{l}]$, $\mathbf{M}_\lambda = [\mathbf{t}\ \ \ln(\mathbf{i})\ \ \mathbf{l}]$ and $\mathbf{M}_{\Delta\lambda} = [\mathbf{t}\ln(\mathbf{t})^{-1}\ \ \sqrt{\mathbf{i}}\ \ \mathbf{l}]$ are all M x 3 basis matrices. $\mathbf{l}$ indicates the M x 1 all-ones vector. $\mathbf{c}_p$, $\mathbf{c}_\lambda$, and $\mathbf{c}_{\Delta\lambda}$ represent 3 x 1 coefficient vectors, each of them could be calculated by linear least square method, e.g., $\mathbf{c}_p = (\mathbf{M}_p^T\mathbf{M}_p)^{-1}\mathbf{M}_p^T\ln(\mathbf{p})$. Appling the above regularized process to $\mathbf{G}^*$ will enable us to find the other set of coefficient vectors ($\mathbf{c_p}$*, $\mathbf{c_\lambda}$*, $\mathbf{c_{\Delta\lambda}}$*). Therefore, the complete spectral function $\tilde{S}(\lambda,T,I)$ at junction temperature (T) and drive current (I) can be posed as:

$$
\begin{aligned}
\tilde{S}(\lambda) &= G + G^* \\
&= \exp[\mathbf{m_p c_p} - (\lambda - \mathbf{m_\lambda c_\lambda})^2 / \exp(\mathbf{m_{\Delta\lambda} c_{\Delta\lambda}})^2] \\
&\quad + \exp[\mathbf{m_p c_p}^* - (\lambda - \mathbf{m_\lambda c_\lambda}^*)^2 / \exp(\mathbf{m_{\Delta\lambda} c_{\Delta\lambda}}^*)^2]
\end{aligned} \tag{5}
$$

where $\mathbf{m_p} = [T\ln(T)\ \ln(I)\ 1]$, $\mathbf{m_\lambda} = [T\ \ \ln(I)\ \ 1]$, and $\mathbf{m_{\Delta\lambda}} = [T\ln(T)^{-1}\ \ \sqrt{I}\ \ 1]$ account for basis vectors with free variables T and I. For the phosphor-converted spectrum, the blue and fluorescence components should be individually considered and also can be decomposed into two double Gaussian functions.

3.2 Multispectral optimization

In colorimetry, metamerism states a phenomenon of matching of an object apparent color with different SPDs. In general lighting the metamerism appears when dealing with the multispectral synthesizing (K-type LED emitters, usually $K > 3$) for a target CIE tristimulus value $\boldsymbol{\varepsilon} = [X\,Y\,Z]^{\mathrm{T}}$. Before adjusting the spectrum of LEDs cluster to approach this target, the current tristimulus value $\tilde{\boldsymbol{\varepsilon}}$ can be described as:

$$\tilde{\boldsymbol{\varepsilon}} = \mathbf{A}\tilde{\mathbf{S}}^{\mathrm{T}}\mathbf{l} \tag{6}$$

where rows of **A** are the sampled color matching functions with dimension N, the K x N spectral matrix $\tilde{\mathbf{S}}$ now contains K-type modeled spectra [from Eq. (5)] extracted N discrete points, and **l** becomes the Kx1 all-ones vector. In this system, two implicit free variables T and I for each type of spectrum make the degrees of freedom turn out to be $2K-3$. Apparently, on this situation it will be time consuming to search an optimal solution to approach $\boldsymbol{\varepsilon}$ and other objectives, i.e. high efficiency and good lighting quality. To solve this issue we assume a localized region including a small number of K-type LEDs has the uniform ambient temperature T_a. This assumption however degenerates the degrees of freedom $2K-3$ into $K-3+1$. On the other hand, we attempt to directly relate the tristimulus value to drive current and have found empirically that a quadratic current basis $\mathbf{i} = [1\ I_1\ \ I_1^2\ I_2\ \ I_2^2 \cdots I_k\ \ I_k^2]^{\mathrm{T}}$ with $(2K+1)$ x 3 coefficient matrix **C** can precisely characterize $\tilde{\boldsymbol{\varepsilon}}$ under a specific T_a. In sum, the Eq. (6) can be rewritten with lower degrees of freedom:

$$\tilde{\boldsymbol{\varepsilon}} = \mathbf{C}^{\mathrm{T}}\mathbf{i} \tag{7}$$

If we now set $\tilde{\boldsymbol{\varepsilon}} = \boldsymbol{\varepsilon}$, an arbitrary current combination will readily be produced by randomly choosing values for $K-3$ currents and then extracting the positive solutions for remained currents. Thus an initial current population, $\mathbf{I_p}$, of "combination changes" with various driving current could be generated. Also the corresponding initial T population, $\mathbf{T_P}$, is obtained. Similarly, the initial SPD population, $\tilde{\mathbf{S}}_{\mathbf{P}}$, comes out via bringing the corresponded T and I in $\mathbf{T_P}$ and $\mathbf{I_p}$ into Eq. (5). To evaluate the performance of the combinations in $\tilde{\mathbf{S}}_{\mathbf{P}}$, at this step, we introduce a user-defined merit function based on the weighted sum method with the figures of merit LE and CQS:

$$f = w \times \mathrm{CQS} + (1-w) \times \mathrm{LE}, \text{ subject to } w \in [0,1] \tag{8}$$

where w modulates the weight between two figures of merit. Imposing each combination in $\tilde{\mathbf{S}}_{\mathbf{P}}$ to Eq. (8) the merit function would lead to a corresponding value; a table of merit function changes vs. $\tilde{\mathbf{S}}_{\mathbf{P}}$, or equivalently, a table of merit function changes vs. $\mathbf{I_p}$, can be established. Afterward we bring the table into a globe searching engine, continuous genetic algorithm, to achieve an improved spectral synthesizing.

4. RESULTS

4.1 Design example

To implement the proposed scheme a pentachromatic high power cluster composed of four single-colors red/amber/green/blue (R/A/G/B/) and a phosphor-converted cool-white (CW) LED is devised (HELIO Optoelectronics Corp., HMHP-E1LW). Figure 3 shows five LED spectra at T_a = 10°C and I = 350mA. An adequate layout of LED arrangement with the consideration of the first-order design delivers a uniform illumination at the center of measurement plane.

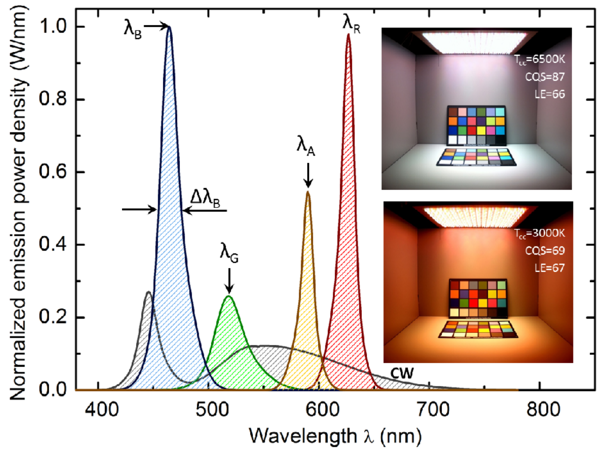

Figure 3. The high power spectra of red (λ_R: 625nm, $\Delta\lambda_R$: 20nm), green (λ_G: 523nm, $\Delta\lambda_G$: 33nm), blue (λ_B: 465nm, $\Delta\lambda_B$: 25nm), amber (λ_A: 587nm, $\Delta\lambda_A$: 18nm) and cool-white LEDs at ambient temperature T_{amb} of 10°C with all I_{dc} of 350mA. The right figures show two real-field tests designed for different color and ambient temperatures.

4.2 Discussion

We firstly exam the temperature dependence of spectra by four cases, T_c = 3200K, 4600K, 6200K, and 7400K distributed over a wild range of color temperature under a specific value of the ambient temperature, T_a = 50°C, as shown in figure 4(a). All cases fulfill the requirements for lighting level = 100 lm, Δxy < 0.01 (T_a = 50°C) and CQS > 85 points with the optimized LE. By changing the ambient temperature without additional compensation and defining the valid bandwidth when chromaticity deviation of Δxy = 0.01, the cluster has relative narrow band (about T_a = 42 °C ~ 56 °C) at lower color temperature range and substantially increases up to around T_a = 25 °C ~ 70 °C at the T_c = 6200K. The chromaticity point shifts toward higher correlated color temperature T_{cc} with the raise of T_a owing to the dramatic deterioration in LEs of the amber and red LEDs as shown in figure 4(b).

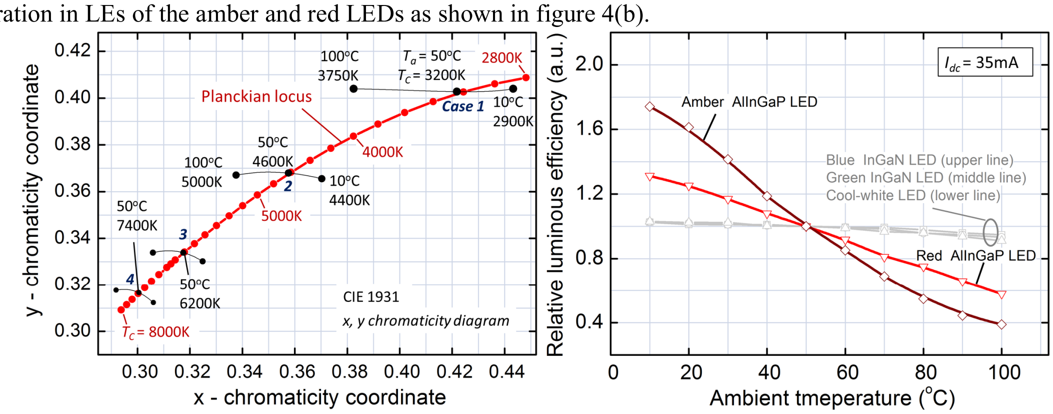

Figure 4. (a) The temperature dependence of spectra designed for T_c = 3200K, 4600K, 6200K, and 7400K at T_a = 50°C. The chromaticity point shifts toward higher color temperature with the raise of T_a owing to the dramatic deterioration in LEs of the red and amber LEDs. (b) The temperature dependence of LE for pentachromatic LEDs. When T_a is varied from 10 °C to 100 °C, LEs of amber and red AlInGaP LEDs decrease to 23% and 46% of that at 10 °C while LEs of InGaP LEDs are insensitive to temperature variation.

In sum, the LE contour map is provided in figure 5 under the compensation for whole operational ambient temperatures. Through the above analysis the best performance (LE > 130 lm/W) appears within the lower T_a region (10 °C ~ 20 °C) with the higher power ratio of the white light emitter (4000K < T_c <6500K), and the worst one happens at the higher T_a region (90 °C ~ 100 °C) with the higher power ratio of the red and amber emitters (2800K < T_c < 3200K). If the LE = 100 lm/W is selected as the minimum acceptable efficiency, a full operational range for T_a is workable when T_c > 5200K.

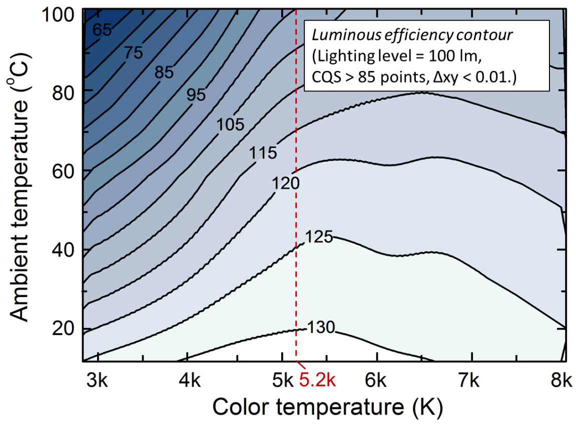

Figure 5. The LE contour of the pentachromatic LEDs cluster. When the LE=100 lm/W is selected as the minimum efficiency boundary, a full operation range for ambient temperature can be obtained for T_c > 5200K.

5. CONCLUSION

A complete high power LEDs mixing scheme has been proposed in consideration of the spectral formalism and the optimization methodology. The phosphor-converted white light can be approximated by simply decomposing the spectrum into two double-Gaussian models developed from single-color spectrum. In the optimization process, the degrees of freedom can be reduced from $2K-3$ to $K-2$ under the localized uniform T_a assumption and the optimal spectral synthesizing can be obtained via incorporating CGA. In order to implement the proposed scheme, a pentachromatic high power cluster is devised. The limitation in operation window at high T_a and low T_c is mainly due to the dramatically deteriorations in luminous efficiency of amber and red light sources, which could be improved by replacing single emitter to two or more ones to share the total emitting power and reduce the thermal effect induced by drive current. While the optimizations for the number of each type LED, prices and whole volume of the cluster need to be further explored. However, the cluster provides a full operable range in ambient temperature when T_c > 5200K by using the proposed scheme, which makes it feasible to provide a high quality smart lighting system that can be efficiently operated within an extended operation range.

REFERENCES

[1] J. K. Kim, and E. F. Schubert, “Transcending the replacement paradigm of solid-state lighting,” Opt. Express 16(26), 21835–21842 (2008), http://www.opticsinfobase.org/oe/abstract.cfm?uri=oe-16-26-21835.

[2] E. F. Schubert, and J. K. Kim, “Solid-state light sources getting smart,” Science 308(5726), 1274–1278 (2005).

[3] E. F. Schubert, Light-emitting Diodes, 2nd ed. (Cambridge University Press, 2006).

[4] Y. Ohno, “Color rendering and luminous efficacy of white LED spectra,” Proc. SPIE 5530, 88–98 (2004).

[5] W. Davis, and Y. Ohno, “Color quality scale,” Opt. Eng. 49(3), 033602 (2010).

[6] M. S. Rea, and J. P. Freyssinier-Nova, “Color rendering: a tale of two metrics,” Color Res. Appl. 33(3), 192–202 (2008).

[7] A. Žukauskas, R. Vaicekauskas, F. Ivanauskas, H. Vaitkevičius, P. Vitta, and M. S. Shur, “Statistical approach to color quality of solid-state lamps,” IEEE J. Sel. Top. Quantum Electron. 15(6), 1753–1762 (2009).

[8] E. F. Schubert, J. K. Kim, H. Luo, and J.-Q. Xi, “Solid-state lighting–a benevolent technology,” Rep. Prog. Phys. 69(12), 3069–3099(2006).

[9] A. Žukauskas, R. Vaicekauskas, F. Ivanauskas, R. Gaska, and M. S. Shur, “Optimization of white polychromatic semiconductor lamps,” Appl. Phys. Lett. 80(2), 234–236 (2002).

[10] G. He, and L. Zheng, “Color temperature tunable white-light light-emitting diode clusters with high color rendering index,” Appl. Opt. 49(24), 4670–4676 (2010).

[11] G. He, and L. Zheng, “White-light LED clusters with high color rendering,” Opt. Lett. 35(17), 2955–2957 (2010).

ACKNOWLEDGMENT

We appreciate the financial support provided by the National Science Council, Taiwan, under grants NSC 99-2221-E-009-067-MY3 and NSC 100-2622-E-009-003-CC2.